Article

Cell Reports

DIXDC1 Phosphorylation and Control of Dendritic Morphology Are Impaired by Rare Genetic Variants

Graphical Abstract

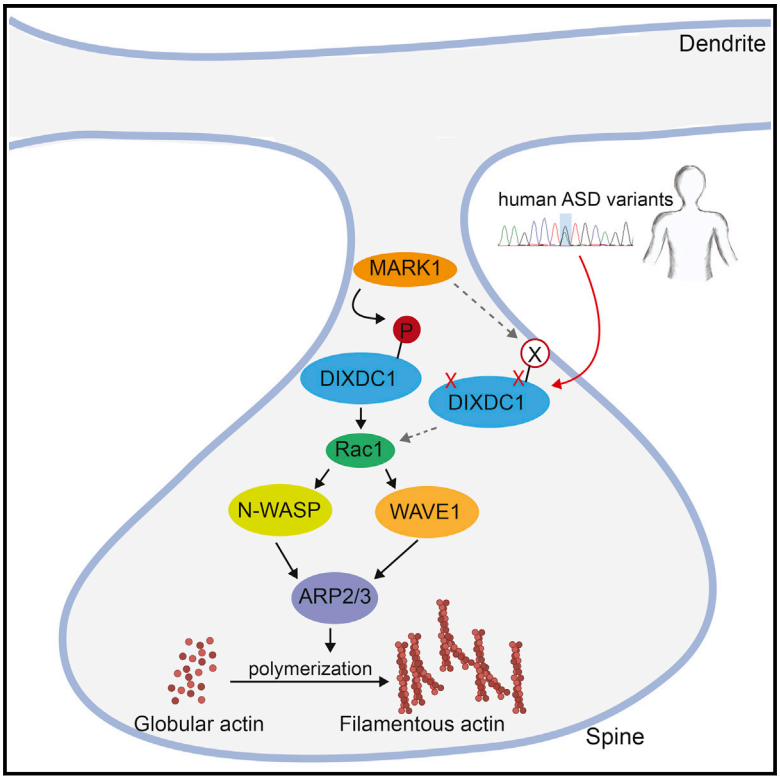

Authors

Vickie Kwan, Durga Praveen Meka, Sean H. White, ..., Stephen W. Scherer, Froylan Calderon de Anda, Karun K. Singh

Correspondence

singhk2@mcmaster.ca

In Brief

Dendritic and synaptic development are important for brain function, and these events are disrupted in individuals with neurodevelopmental disorders. Kwan et al. show that MARK1-dependent phosphorylation of DIXDC1 regulates cortical neuron dendrite and spine morphogenesis through a cytoskeletal pathway that is disrupted by rare genetic variants identified in autism cohorts.

Highlights

- DIXDC1 is a regulator of dendrite and spine development
- MARK1 phosphorylates DIXDC1 isoforms to regulate dendrite and spine development
- Phosphorylation of DIXDC1 isoform 1 regulates cytoskeletal dynamics
- ASD variants in DIXDC1 isoform 1 impair phosphorylation and neuronal morphology

Kwan et al., 2016, Cell Reports *17*, 1892–1904
November 8, 2016
http://dx.doi.org/10.1016/j.celrep.2016.10.047

OPEN ACCESS
CellPress

Cell Reports
Article

DIXDC1 Phosphorylation and Control of Dendritic Morphology Are Impaired by Rare Genetic Variants

Vickie Kwan,[1,2] Durga Praveen Meka,[3] Sean H. White,[1,2] Claudia L. Hung,[2] Nicholas T. Holzapfel,[1,2] Susan Walker,[4,5] Nadeem Murtaza,[1,2] Brianna K. Unda,[1,2] Birgit Schwanke,[3] Ryan K.C. Yuen,[4,5] Kendra Habing,[1,2] Chloe Milsom,[1,2] Kristin J. Hope,[1,2] Ray Truant,[2] Stephen W. Scherer,[4,5] Froylan Calderon de Anda,[3] and Karun K. Singh[1,2,6,*]

[1]Stem Cell and Cancer Research Institute
[2]Department of Biochemistry and Biomedical Sciences, Michael G. DeGroote School of Medicine
Faculty of Health Sciences, McMaster University, Hamilton, ON L8N 3Z5, Canada
[3]Center for Molecular Neurobiology Hamburg (ZMNH), University Medical Center Hamburg-Eppendorf, Falkenried 94, 20251 Hamburg, Germany
[4]The Centre for Applied Genomics and Program in Genetics and Genome Biology, The Hospital for Sick Children, Peter Gilgan Centre for Research and Learning, Toronto, ON M5G 0A4, Canada
[5]Department of Molecular Genetics and McLaughlin Centre, University of Toronto, Toronto, ON M5S 1A1, Canada
[6]Lead Contact
*Correspondence: singhk2@mcmaster.ca
http://dx.doi.org/10.1016/j.celrep.2016.10.047

SUMMARY

The development of neural connectivity is essential for brain function, and disruption of this process is associated with autism spectrum disorders (ASDs). DIX domain containing 1 (*DIXDC1*) has previously been implicated in neurodevelopmental disorders, but its role in postnatal brain function remains unknown. Using a knockout mouse model, we determined that DIXDC1 is a regulator of excitatory neuron dendrite development and synapse function in the cortex. We discovered that MARK1, previously linked to ASDs, phosphorylates DIXDC1 to regulate dendrite and spine development through modulation of the cytoskeletal network in an isoform-specific manner. Finally, rare missense variants in *DIXDC1* were identified in ASD patient cohorts via genetic sequencing. Interestingly, the variants inhibit DIXDC1 isoform 1 phosphorylation, causing impairment to dendrite and spine growth. These data reveal that DIXDC1 is a regulator of cortical dendrite and synaptic development and provide mechanistic insight into morphological defects associated with neurodevelopmental disorders.

INTRODUCTION

Dendritic spines are the primary sites of excitatory synaptic inputs and are necessary for cognitive function (Ebert and Greenberg, 2013; Jeste and Geschwind, 2014; Penzes et al., 2011). The importance of spines is revealed by their disruption in individuals with autism spectrum disorders (ASDs) (Tang et al., 2014) and the identification of ASD-linked mutations in synaptic genes (Chen et al., 2015; De Rubeis et al., 2014; Geschwind and State, 2015; Iossifov et al., 2014). One mechanism that causes synaptic dysfunction in disease is disruption of the cytoskeletal network (De Rubeis et al., 2013; Dolan et al., 2013; Duffney et al., 2013; Durand et al., 2012; Han et al., 2013; Hori et al., 2014), which includes abnormalities in actin and tubulin dynamics (De Rubeis et al., 2013; Gu et al., 2010; Lei et al., 2016; Muhia et al., 2016; Murakoshi et al., 2011; Um et al., 2014; Woolfrey and Srivastava, 2016). Interestingly, cytoskeleton-based synaptic defects in ASD mouse models can be pharmacologically reversed, suggesting a potential therapy (Dolan et al., 2013; Duffney et al., 2015; Huang et al., 2013).

Wingless (Wnt) signaling has also been linked to ASDs and psychiatric disorders (Cao et al., 2016; Kalkman, 2012; Krumm et al., 2014; Martin et al., 2013; Okerlund and Cheyette, 2011). Mouse model and human induced pluripotent stem cell (iPSC) studies have demonstrated that altered Wnt signaling causes disease phenotypes (Brennand et al., 2011; Fang et al., 2014; Mohn et al., 2014; Okerlund et al., 2010; Sowers et al., 2013; Srikanth et al., 2015; Topol et al., 2015). The Wnt and synaptic pathways also intersect and include molecules, such as Dishevelled-1, Dact1, β-catenin, DISC1, Ankyrin G, and APC, indicating that Wnt molecules have important roles at the synapse (Ciani et al., 2015; Hayashi-Takagi et al., 2010, 2014; Mao et al., 2009; Okerlund et al., 2010; Sowers et al., 2013; Srikanth et al., 2015; Turner et al., 2015; Wen et al., 2014).

The link between Wnt signaling and ASDs prompted us to study whether DIXDC1 regulates the development of neural connectivity. DIXDC1 regulates embryonic neural progenitor cell proliferation and cerebellar axonal growth (Ikeuchi et al., 2009; Shiomi et al., 2003, 2005; Singh et al., 2010; Soma et al., 2006), but there is no known role for DIXDC1 in postnatal cortical development. DIXDC1 has been linked to psychiatric disorders (Singh et al., 2010), and a *Dixdc1* knockout (KO) mouse model displays behavioral deficits (Kivimäe et al., 2011). DIXDC1 can be phosphorylated and recruited to focal adhesions by microtubule-associated protein (MAP)/microtubule affinity-regulating

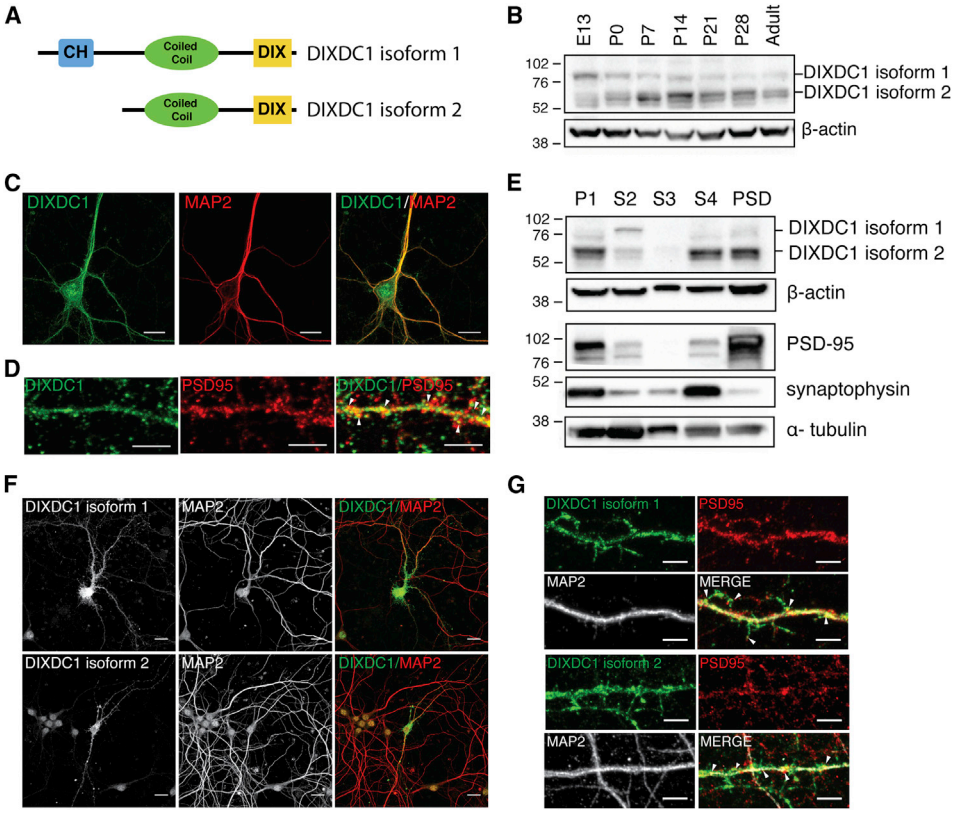

Figure 1. Characterization and Localization of DIXDC1

(A) Schematic diagram of DIXDC1 protein structure.

(B) Western blot analysis of mouse brain lysates probed for DIXDC1 (actin-loading control).

(C) DIV14 cortical neuron cultures show localization of DIXDC1, co-stained for microtubule-associated protein 2 (MAP2).

(D) DIV14 cortical neurons were immunostained and show co-localization of DIXDC1 with PSD95 (arrows).

(E) Postsynaptic densities (PSD) fractionated from P28 mouse brains were probed for DIXDC1, actin, PSD95, synaptophysin, and tubulin. P1, nuclear fraction; PSD, post synaptic density; S2, crude cytoplasm; S3, crude synaptic vesicle; S4, crude synaptosomal membrane fraction.

(F and G) Immunostained DIV14 mouse cultures show co-localization of GFP-tagged DIXDC1 isoforms 1 and 2 with PSD95 and MAP2 (arrows).

All numerical data are given as mean ± SEM. The scale bars represent 20 μm for (C) and (F) and 5 μm for (D) and (G). See also Figure S1.

kinase 1 (MARK1) in human osteosarcoma cell lines (Goodwin et al., 2014), suggesting that DIXDC1 could regulate the cytoskeleton in neurons. Interestingly, MARK1 regulates hippocampal synaptic growth (Wu et al., 2012) and has been linked to ASDs (Maussion et al., 2008), suggesting it might partner with DIXDC1 to regulate synaptic development.

Given these observations, we explored whether DIXDC1 regulates postnatal cerebral cortex development. We found phosphorylation of DIXDC1 isoforms 1 and 2 by MARK1 is required for dendrite and spine growth; however, the modulation of the neuronal cytoskeleton was specifically mediated by DIXDC1 isoform 1. We also identified inherited, rare missense variants in *DIXDC1* from genetic sequencing of ASD patient cohorts and discovered they reduce phosphorylation of DIXDC1 isoform 1 and impair neuronal morphology. Our data reveal that MARK1-DIXDC1 signaling is a critical regulator of dendrite and synaptic development and outline how rare genetic variants in *DIXDC1* may contribute to altered neuronal morphology during brain development.

RESULTS

Expression of DIXDC1 in Neurons

The embryonic expression of DIXDC1 in the brain has been previously described (Shiomi et al., 2003, 2005; Singh et al., 2010). Therefore, we probed brain lysates from multiple ages for DIXDC1 isoforms 1 and 2 (Figure 1A) and found that both isoforms are expressed postnatally (Figure 1B). We also stained 14 days in vitro (DIV14) cultured cortical neurons and found that DIXDC1 is expressed in MAP2-positive dendrites (Figure 1C) and partially co-localizes with postsynaptic density 95 (PSD95) (Figure 1D). Biochemical isolation of the postsynaptic density (PSD) also revealed that both DIXDC1 isoforms are present (Figure 1E). Finally, we tagged each DIXDC1 isoform with GFP and found that both isoforms are expressed in dendrites and spines (Figures 1F and 1G) and both partially co-localize with PSD95 (Figure 1G). Together, these data indicate that both isoforms localize to dendrites and spines and may regulate neuronal morphogenesis.

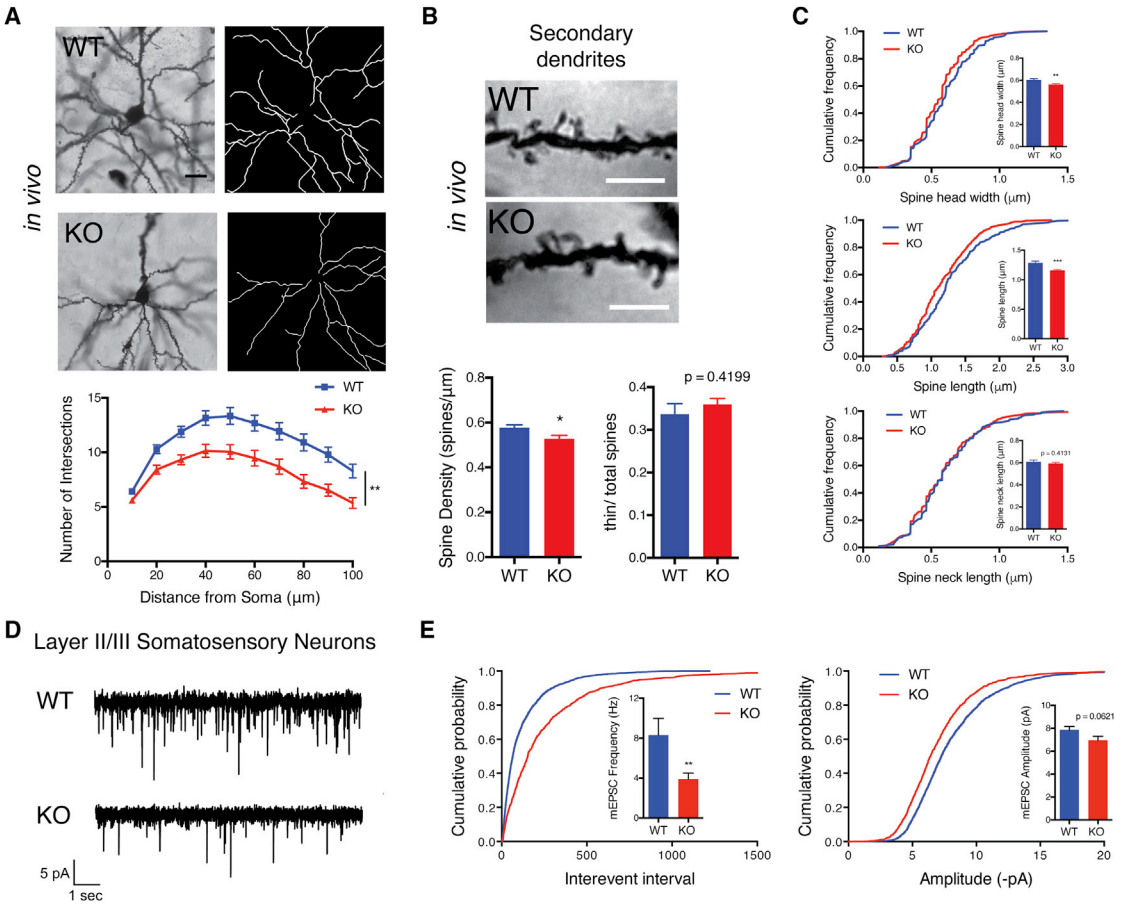

Figure 2. DIXDC1 Is Required for Dendrite Growth and Dendritic Spine Function

(A) Golgi-stained layers 2/3 somatosensory neurons from cortex in WT or *Dixdc1* KO mice (P28). Sholl analysis reveals KO mice display a decrease in dendrite complexity (n = 3 mice; two-way ANOVA; post hoc Sidak test: $^{**}p < 0.01$). See Supplemental Information for detailed statistical methods.

(B) Morphological analysis of P28 layers 2/3 somatosensory secondary dendrites in *Dixdc1* KO neurons shows decreased spine density and increased thin spines compared to WT neurons (n = 3 mice; t test: $^{*}p < 0.05$).

(C) Morphological analysis of spine head width, spine length, and spine neck length (μm) distribution. Spine head width and spine length were decreased in *Dixdc1* KO neurons (n = 3 mice; t test: $^{**}p < 0.01$; $^{***}p < 0.001$; p values for specific distances in Supplemental Information).

(D) Loss of DIXDC1 reduces excitatory synaptic function. Representative traces of recorded mEPSCs from KO mouse (bottom) and WT control brain slices (top; n > 4 mice).

(E) KO mice display a significantly reduced mEPSC frequency (two-tailed Mann Whitney U-test: $^{**}p < 0.01$) with no change in amplitude. Cumulative probability of mEPSC frequency and amplitude shows spine head width and spine length was significantly decreased in KO (n > 4 mice; Kolmogorov-Smirnov t test: $^{****}p < 0.0001$).

All numerical data are given as mean ± SEM. The scale bars represent 20 μm for (A) and 5 μm for (B). See also Figures S2–S4.

Dixdc1 KO Mice Have Defects in Dendrite and Spine Development

To study DIXDC1, we obtained a complete *Dixdc1* KO mouse (Figures 3E and S1A). Assessment of cortical structure using a layer-specific marker revealed no gross differences (Figure S1B). In 4-week-old KO mice, we determined that layer 2/3 somatosensory cortical pyramidal neurons had significantly reduced dendrite complexity compared to WT (Figure 2A). To corroborate these data, we cultured *Dixdc1* KO neurons and found a significant reduction in dendrite complexity (Figure 4A). As a control, we acutely knocked down *Dixdc1* using short hairpin RNA (shRNA) both in vivo and in vitro and found a significant reduction in dendrite complexity (Figures S2A–S2C), which was rescued by an shRNA-resistant human DIXDC1 (Figure S2D). These studies suggest that DIXDC1 is required for dendrite growth in a cell-autonomous fashion.

Given the expression of DIXDC1 isoforms at the PSD, we postulated DIXDC1 regulates spine structure. We imaged spines in P28 layer 2/3 cortical neurons from KO mice and found a modest but significant reduction in spine density compared to WT (Figure 2B). Additional analysis showed a decrease in spine head width and length in KO mice (Figure 2C). In vitro experiments confirmed that KO neurons had significantly reduced spine density but no changes in thin spines (Figure 4B). Furthermore, acute knockdown of *Dixdc1* in vitro and in vivo revealed

a significant decrease in spine density, which was rescued by shRNA-resistant human DIXDC1 (Figures S2E–S2G). We included an additional control experiment and knocked down *Dixdc1* after dendrite growth, which also revealed a decrease in spine density, indicating that DIXDC1 specifically regulates spine structure (Figure S2H).

DIXDC1 Regulates the Development of Synaptic Connectivity and Function

Considering the reductions in dendritic complexity, spine density, and spine size in *Dixdc1* KO mice, we examined whether this altered synapse activity, using electrophysiology. We recorded from layer 2/3 cortical neurons within the somatosensory cortex (Figure 2D) and observed a significant reduction in miniature excitatory postsynaptic current (mEPSC) frequency in KO animals compared to WT controls (Figure 2E). Despite a trend toward a reduction in spine size in KO neurons, there were no significant differences in mEPSC amplitude (Figure 2E). Given these data, we also examined the morphological development of synapses using the presynaptic marker synaptophysin. Quantification revealed that reducing DIXDC1 expression significantly reduced synaptophysin puncta density (Figure S3A). Lastly, we measured in vitro neural connectivity using a genetically encoded rabies virus that allows fluorescent visualization of monosynaptic connections (Garcia et al., 2012). Using this assay, we found that individual neurons lacking DIXDC1 had a reduced number of monosynaptic connections with neighboring neurons (Figure S3B). Taken together, these multiple lines of investigation suggest DIXDC1 is required for synaptic connectivity and function.

MARK1 Phosphorylates DIXDC1 in the Brain

Our data indicate that DIXDC1 regulates dendrite and synapse formation; however, the mechanism(s) involved are unknown. MARK1 phosphorylates DIXDC1 isoform 1, which causes localization to actin-rich focal adhesions in cell lines (Figure 3A; Goodwin et al., 2014), suggesting the possibility that DIXDC1 regulates the cytoskeleton in neurons. We first tested the expression pattern of MARK1 in the brain and found its developmental profile is similar to DIXDC1 (Figure 3B). We also found that MARK1 co-localizes with DIXDC1 in dendrites (Figure 3C) and was enriched in the PSD (Figure 3D), indicating that MARK1 could phosphorylate DIXDC1.

To test this, we expressed MARK1-wild-type (WT) with hDIXDC1-WT isoform 1 or isoform 2 in HEK293 cells and found robust phosphorylation of both DIXDC1 isoforms (Figures 3F and 3G), which was inhibited by a substitution of serine-592 to alanine (S592A) in isoform 1 or a S381A mutation in isoform 2 (Figures 3F and 3G). Next, we examined whether either DIXDC1 isoform was endogenously phosphorylated in vivo. We probed mouse brain lysate and found that both DIXDC1 isoforms are phosphorylated, which was eliminated in the KO mouse (Figure 3E). These data demonstrate that MARK1 phosphorylates both DIXDC1 isoforms in the brain.

Phosphorylation of DIXDC1 Is Required for Dendrite and Spine Growth

Given that MARK1 phosphorylates DIXDC1, we asked whether this regulates dendrite and spine growth. First, we co-transfected WT cultured neurons with GFP and a specific isoform of DIXDC1. We found that WT hDIXDC1 isoforms 1 and 2 both individually increased dendrite branching (Figure S4A) and spine density (Figure S4B). We also tested mouse Dixdc1 (isoform 1) and found the same effect (Figures S4C and S4D). We next expressed each DIXDC1 isoform in KO neurons and determined that expression of either isoform significantly increases (rescues) dendrite growth and spine formation (Figures 4C–4F). These data imply that both DIXDC1 isoforms play a prominent role in dendrite and spine growth.

To determine the role of MARK1 phosphorylation of DIXDC1 in dendrite and spine formation, we expressed phospho-mutant versions of each isoform into cultured *Dixdc1* KO neurons. Overexpression of hDIXDC1-S592A (isoform 1) or hDIXDC1-S381A (isoform 2) did not increase dendrite growth or spine density in KO cultures (Figures 4C–4F). This suggests that phosphorylation is required for dendrite growth and spine formation. Next, we expressed both phospho-dead isoforms of DIXDC1 in the WT background to determine whether they possess dominant-negative activity. For isoform 1, hDIXDC1-S592A did not function similar to hDIXDC1-WT and caused a decrease in dendrite branching even compared to controls, whereas spine density was not significantly different than WT isoform 1 (Figures S5A and S5C). For isoform 2, the phospho-mutant (S381A) did not increase dendrite growth or spine density compared to WT and was similar to GFP controls (Figures S5B and S5D). This indicates phospho-dead isoform 1, but not isoform 2, possesses some dominant-negative activity. As a control, we found no gross differences in expression of the mutants (Figure S6A).

We also examined whether phosphorylation of DIXDC1 was important for its localization in dendrites and spines. Cultured cortical neurons showed co-localization of GFP-tagged hDIXDC1-WT (isoforms 1 and 2) with PSD95 in the dendritic spines (Figures 4G and 4H). However, the hDIXDC1-S592A and -S381A phospho-mutants both exhibited a decrease in PSD95 co-localization, indicating DIXDC1 localization to spines was disrupted (Figures 4G and 4H). These results strongly indicate that phosphorylation of both DIXDC1 isoforms is critical for cortical dendrite and synapse formation.

Phosphorylation of DIXDC1 Regulates Actin and Microtubule Cytoskeletal Dynamics

Previous studies suggest that DIXDC1 may directly impact the cytoskeleton, which could influence dendrite and spine growth (Capelluto et al., 2002; Singh et al., 2010; Wang et al., 2006). We first examined actin integrity in vivo and found that *Dixdc1* KO brains had a significant reduction in the F-/G-actin ratio (Figure 5A). We next analyzed the levels of proteins that regulate actin polymerization and observed a significant decrease in Rac1-GTP activity, but not Rho-GTP levels in KO brains (Figure 5B). We also found a significant reduction in the Wiskott-Aldrich syndrome proteins WAVE-2, N-WASP, as well as Profilin-1 (Figure 5C). These observations suggest that DIXDC1 regulates actin polymerization in the brain. To investigate whether a defect in actin polymerization causes the spine phenotype in *Dixdc1* KO neurons, we enhanced actin polymerization using Jasplakinolide (JPK) (Reinhard et al., 2016). We found that JPK significantly increased dendritic spine density in KO cultures to levels similar

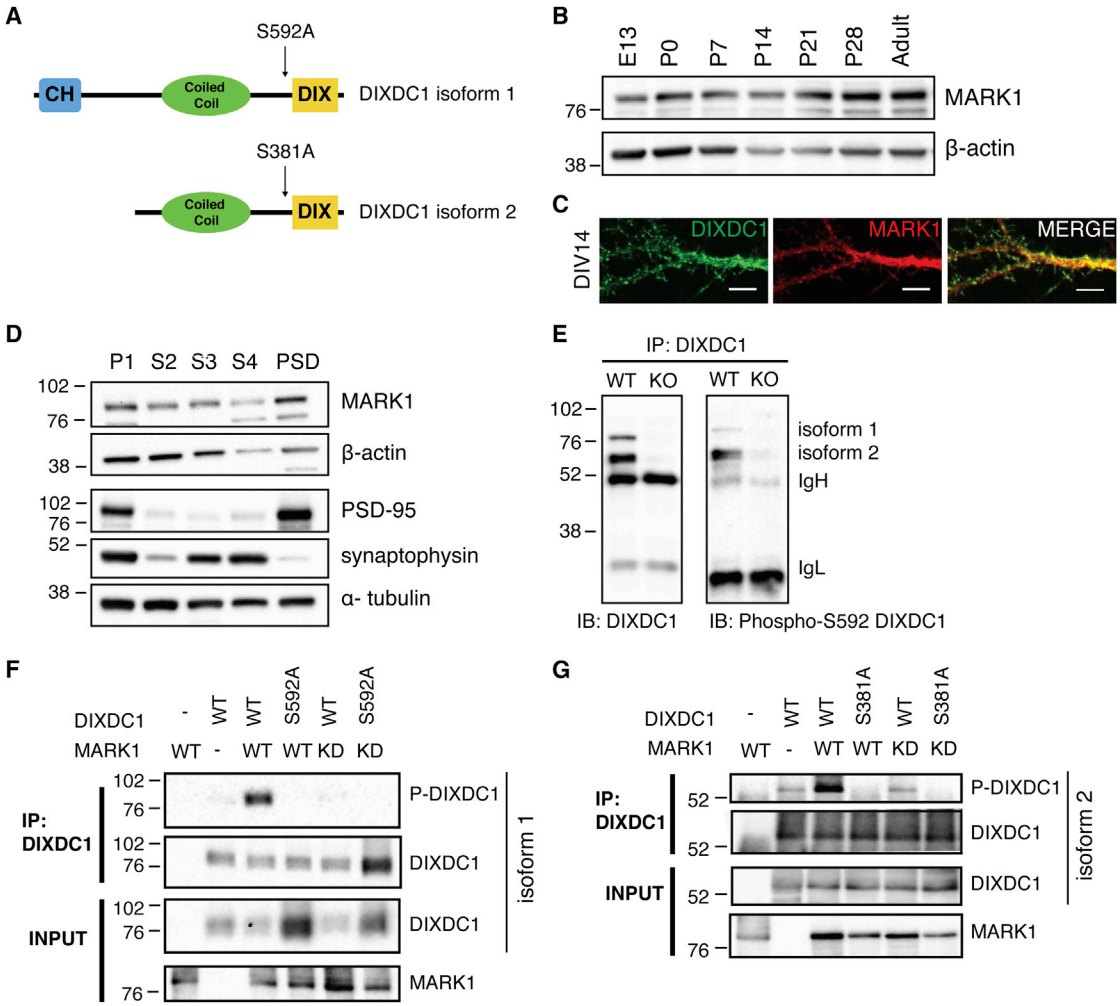

Figure 3. MARK1 Phosphorylates DIXDC1 at Serine 592/381 in the Brain

(A) Schematic diagram of MARK1 phosphorylation site at serine 592 of hDIXDC1 isoform 1 and at serine 381 of hDIXDC1 isoform 2.

(B) Western blot analysis of a time course of CD-1 mouse brain lysates, probed for MARK1 (actin-loading control).

(C) DIV14 cultured WT cortical neurons were immunostained for DIXDC1 and MARK1 and show co-localization in dendrites.

(D) Postsynaptic densities (PSDs) fractionated from 1-month-old CD-1 mouse brains probed for MARK1, actin, PSD95, synaptophysin, and tubulin. P1, nuclear fraction; S2, crude cytoplasm; S3, crude synaptic vesicle; S4, crude synaptosomal membrane fraction; PSD, post synaptic density.

(E) Immunoprecipitation of 1-month-old WT and *Dixdc1* KO mouse brain with anti-DIXDC1 antibody and then probed for DIXDC1 (left) and phospho-Ser592 DIXDC1 (right).

(F) HEK293FT cells transfected with MARK-WT or T215A (kinase dead [KD]) and hDIXDC1-WT (isoform 1) or hDIXDC1-S592A (phosho-dead; SA). DIXDC1 was immunoprecipitated and probed for p-DIXDC1 S592 and DIXDC1.

(G) HEK293FT cells transfected with MARK-WT or -KD and hDIXDC1-WT or -S381A (isoform 2). DIXDC1 was immunoprecipitated and probed for p-DIXDC1 S592/S381 and DIXDC1.

The scale bar represents 5 μm for (C).

to WT cultures treated with JPK (Figure 5D). Importantly, JPK treatment decreased the proportion of thin spines, suggesting that it increases the number of mature, functional spines.

We next explored whether phosphorylation of DIXDC1 regulates the actin cytoskeleton. We monitored actin dynamics in DIV2–3 hippocampal neurons due to the reliability for live imaging at this age and used Lifeact-GFP to monitor actin (Riedl et al., 2008, 2010; Figures 5F and S6E; Movies S1, S2, S3, S4, and S5). Interestingly, we found that WT-DIXDC1 isoform 1, but not isoform 2, significantly alters F-actin retrograde speed (Figures 5F and 5G). Furthermore, both the hDIXDC1-S592A (isoform 1) and -S381A (isoform 2) mutants were different than their WT counterparts with respect to their impact on retrograde speed, suggesting the isoforms differentially regulate actin (Figures 5F and 5G). We also found the percentage of neurites with an intact growth cone was reduced in neurons expressing hDIXDC1-S592A (isoform 1) or hDIXDC1-S381A (isoform 2), indicating that MARK1 phosphorylation is required for actin integrity (Figure 5I). JPK treatment was found to increase spine density and reduce the number of thin spines in neurons expressing

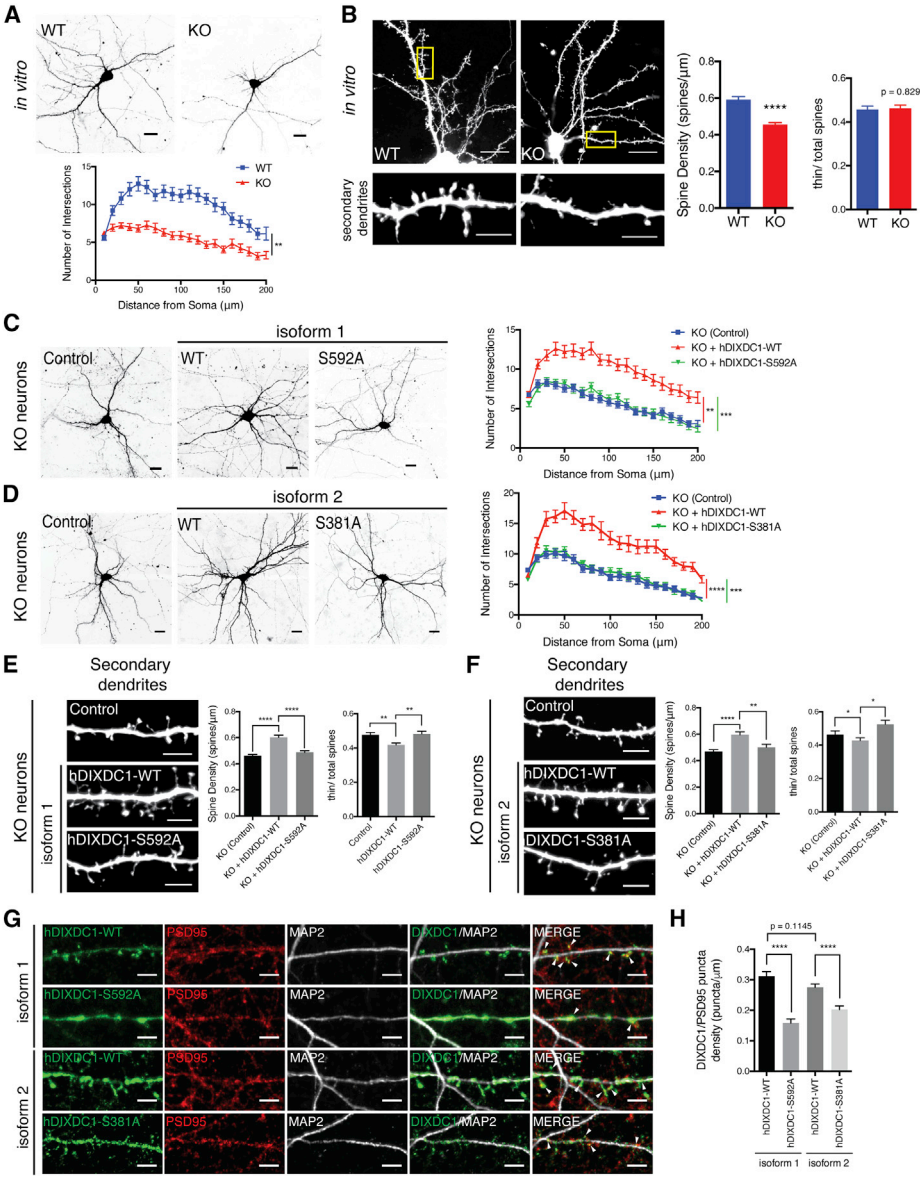

Figure 4. Phosphorylation of DIXDC1 Isoforms by MARK1 Regulates Neuronal Morphology

(A) Sholl analysis of cultured DIV14 WT and *Dixdc1* KO neurons shows a decrease in dendrite complexity in *Dixdc1* KO neurons (n = 4 cultures; two-way ANOVA test: $^{**}p < 0.01$).

(B) Spine morphological analysis of cultured WT and *Dixdc1* KO neurons showed a decrease in spine density in *Dixdc1* KO neurons at DIV14 (n = 3 cultures; t test: $^{****}p < 0.0001$).

(C) Sholl analysis of overexpression of hDIXDC1-S592A (isoform 1) in *Dixdc1* KO cultures demonstrates no rescue in dendrite growth defects (n = 4 cultures; two-way ANOVA; post hoc Sidak test: $^{**}p < 0.01$; $^{***}p < 0.001$).

(D) Sholl analysis of overexpressed hDIXDC1-S381A (isoform 2) in *Dixdc1* KO cultures was unable to rescue dendrite growth defects (n = 3 cultures; two-way ANOVA; post hoc Sidak test: $^{***}p < 0.001$; $^{****}p < 0.0001$).

(E) Spine analysis reveals that overexpression of hDIXDC1-S592A (isoform 1) in *Dixdc1* KO cultures does not increase dendritic spine density (n = 3 cultures; one-way ANOVA; post hoc Sidak test: $^{**}p < 0.01$; $^{****}p < 0.0001$).

(F) Spine analysis of overexpressed hDIXDC1-S381A (isoform 2) in *Dixdc1* KO cultures does not increase dendritic spine density (n = 3 cultures; one-way ANOVA; post hoc Sidak test: $^{*}p < 0.05$; $^{**}p < 0.01$; $^{****}p < 0.0001$).

(G) Cortical neurons transfected with GFP-tagged hDIXDC1-WT, -S592A (isoform 1), hDIXDC1-WT, or -S381A (isoform 2) and were immunostained with antibodies against GFP, PSD95, and MAP2. Arrows show co-localization of DIXDC1 isoforms 1 and 2 with PSD95.

(H) Quantification of DIXDC1 and PSD95 co-localization puncta density on MAP2-positive secondary dendrites (n = 3 cultures; one-way ANOVA; post hoc Sidak test: $^{****}p < 0.0001$).

All numerical data are given as mean ± SEM. The scale bars represent 20 μm for (A), (C), and (D) and 5 μm for (B), (E), (F), and (G). See also Figure S5. Refer to Supplemental Experimental Procedures and Figure S8 for details on image acquisition and analysis.

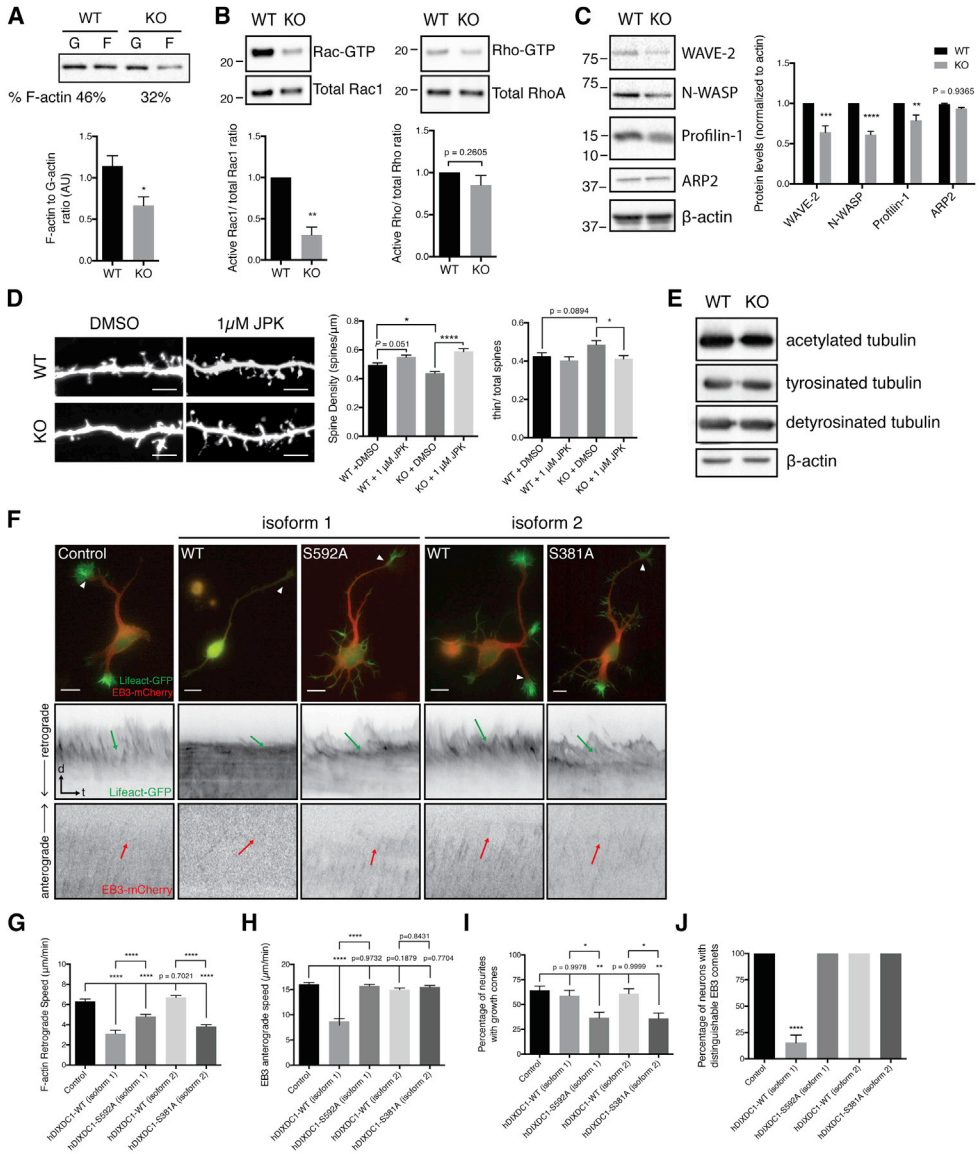

Figure 5. Phosphorylation of DIXDC1 Regulates Cytoskeleton Dynamics and Spine Growth

(A) F- to G-actin ratio was biochemically assayed in P30 WT and *Dixdc1* KO mice. KO brains have a decreased level of F-/G-actin compared to WT mice (n = 3 mice; t test: *p < 0.05).

(B) Active Rac1 and active RhoA levels were measured in WT and KO brains, and KO brains have decreased level of Rac1-GTP/total Rac1 (n = 3 mice; t test: *p < 0.05).

(C) WT and KO whole-brain lysates (P28) were probed for WAVE-2, N-WASP, and profilin-1 levels and show a decrease in all three proteins (n = 3 mice; Wilcoxon signed-rank test: **p < 0.01; ***p < 0.001; ****p < 0.0001).

(D) DIV14 cultured WT and *Dixdc1* KO cortical neurons treated with 1 μM JPK and assessed morphologically. JPK increased dendritic spine density in KO cultures, similar to treated WT cultures (n = 3 cultures; one-way ANOVA; post hoc Sidak test: *p < 0.05; ****p < 0.0001).

(E) WT and KO whole-brain lysates (P30) were probed for acetylated tubulin, tyrosinated tubulin, and detyrosinated tubulin.

(F) Cultured rat hippocampal neurons (DIV2) transfected with Lifeact-GFP and EB3-mCherry, and hDIXDC1-WT, or -S592A (isoform 1), or hDIXDC1-WT, -S381A (isoform 2). Kymographs were generated from time-lapse videos. White arrows show the representative neurite. Green arrows show the speed of F-actin comets, and red arrows show the speed of EB3 comets.

(G) hDIXDC1-WT isoform 1 alters F-actin retrograde speed. Both hDIXDC1-S592A and -S381A showed similar changes in F-actin speeds (n = 3 cultures; one-way ANOVA; post hoc Sidak test: ****p < 0.0001).

(H) hDIXDC1-WT isoform 1 EB3 anterograde speeds were decreased compared to control neurons (n = 3 cultures; one-way ANOVA; post hoc Sidak test: ****p < 0.0001).

(I) Quantification of the percentage of neurites with growth cones in the indicated conditions (n = 3 cultures; one-way ANOVA; post hoc Sidak test: *p < 0.05; **p < 0.01).

(J) Quantification of the percentage of neurons with EB3 comets (n = 3 cultures; one-way ANOVA; post hoc Sidak test: ****p < 0.0001).

All numerical data are given as mean ± SEM. The scale bars represent 10 μm for (F) and 5 μm for (E). See also Figure S6 and Movies S1, S2, S3, S4, and S5.

Table 1. Rare Missense Variants in *DIXDC1* Discovered through Whole-Genome Sequencing of Canadian ASD Cohorts; Summary of Rare Missense Variants in *DIXDC1* from Canadian Simplex Families

Chromosome	Position (Begin)	Reference Allele	Child Genotype	Amino Acid Change	Inheritance	1,000 g_all	NHLBI_all	dbSNP	PolyPhen Score	Number of Cases
chr11	111,808,246	G	G/A	G8E	paternal	NA	NA	NA	0.998	1
chr11	111,835,339	G	G/A	V43M	paternal	NA	NA	NA	0.999	2
chr11	111,859,774	A	A/T	I370L	maternal	NA	0.000254	rs373126732	0.946	1
chr11	111,887,493	C	C/T	T612M	paternal	0.0014	0.000659	rs184718561	1.0	2

hDIXDC1-S592A isoform 1 or hDIXDC1-S381A isoform 2 to levels comparable to JPK-treated WT neurons (Figures S6C and S6D). This demonstrates that enhancing actin polymerization improves spine deficits caused by the phosphorylation mutations.

We also examined whether DIXDC1 regulates the microtubule network using live imaging of red fluorescent protein (RFP)-tagged EB3 in the same neurons expressing Lifeact-GFP (Figure 5F). We found that hDIXDC1-WT (isoform 1) significantly alters EB3 anterograde comet speed and the number of neurons with comets (Figures 5F, 5H, and 5J), whereas isoform 2 had no effect, indicating that isoform 1 preferentially modulates the microtubule network. Furthermore, hDIXDC1-S592A (isoform 1) had no effect on EB3 comet movements, demonstrating that MARK1-mediated phosphorylation of isoform 1 regulates the microtubule network (Figures 5F, 5H, and 5J). Measurements of global microtubule modifications revealed no overt differences (Figure 5E). Overall, these data indicate that DIXDC1 isoform 1 is the predominant isoform that regulates the actin and microtubule cytoskeleton in neurons.

Rare Missense Variants in *DIXDC1* Impair Phosphorylation of Isoform 1 and Inhibit Dendrite and Spine Growth

Finally, we investigated whether there was a functional link between DIXDC1 and ASD. We examined whole-genome sequence data for a cohort of individuals with ASD extracted from the MSSNG database (https://www.mss.ng/researchers#; Yuen et al., 2015). We discovered four rare inherited variants in *DIXDC1* isoform 1: glycine-8 to glutamic acid (G8E); valine-43 to methionine (V43M); isoleucine-370 to leucine (I370L; I159L in isoform 2); and threonine-612 to methionine (T612M; T401M in isoform 2; Table 1). The V43M and T612M variants were found in two independent probands and validated (Figures 6A and S7C). As a control, we did not find changes in variant expression levels in cells (Figure S6B).

We first asked whether the variants impaired DIXDC1 phosphorylation. We overexpressed the variants (V43M and T612M for isoform 1; T401M for isoform 2) into HEK293 cells with MARK1. To our surprise, we discovered that only the variants in DIXDC1 isoform 1 (not isoform 2) significantly impaired phosphorylation by MARK1 (Figures 6B and 6C). We next determined whether dendrite and spine formation is impaired by the variants in isoform 1. We found that the hDIXDC1-V43M and -T612M isoform 1 variants were unable to increase (rescue) dendrite branching or spine density in KO neurons, suggesting a loss of function (Figures 6D and 6E). Additionally, we expressed the isoform 1 variants in WT cortical neurons and found that hDIXDC1-V43M did not increase dendrite complexity compared to hDIXDC1-WT, suggesting it is a loss-of-function variant (Figure S7A). The C-terminal T612M isoform 1 variant also disrupted dendrite complexity, and it displayed dominant-negative activity (Figure S7A). Dendritic spine analysis revealed that both isoform 1 variants (V43M and T612M) were unable to significantly increase spine density compared to hDIXDC1-WT isoform 1 in WT neuronal cultures and were no different than controls (Figure S7B). Finally, JPK treatment of the hDIXDC1 isoform 1 V43M and T612M variants increased dendritic spine density, indicating that the dendritic spine defects are reversible (Figure 6F). Taken together, these data suggest that rare missense variants in *DIXDC1* isoform 1 impair phosphorylation by MARK1, leading to abnormal development of neuronal morphology through a cytoskeleton-based mechanism.

DISCUSSION

The mechanism by which genes associated with neurodevelopmental disorders impact brain development remains poorly understood. We reveal that *DIXDC1* isoforms regulate the morphological development of cortical excitatory neurons and demonstrate that MARK1 phosphorylation of DIXDC1 is required for dendrite and spine growth. Furthermore, we identify isoform-specific roles for DIXDC1, determining that isoform 1 predominantly regulates the cytoskeleton in neurons. Finally, rare missense variants found in *DIXDC1* from ASD individuals impair DIXDC1 isoform 1 phosphorylation, leading to dendrite and spine growth defects. These data delineate how a MARK1-DIXDC1 signaling pathway underlies the development of synaptic connectivity and reveal a mechanism whereby rare genetic variants have a detrimental biological impact.

DIXDC1 Isoform-Specific Regulation of Dendrite Formation and Spine Morphology

Whereas both DIXDC1 isoforms regulates dendrite and spine growth, we detected isoform-specific effects. Both DIXDC1 isoforms can localize to dendrites and synapses and rescue defects in *Dixdc1* KO cultures. However, the mechanism of action of each isoform is different because we detected a clear ability of isoform 1, but not isoform 2, to modulate the cytoskeleton. We also delineated a signaling pathway downstream of DIXDC1 that accounts for this, a Rac1-WAVE-2/N-WASP signaling cascade that regulates F-actin polymerization. Functional analysis of the C-terminal MARK1-phosphorylation site indicates

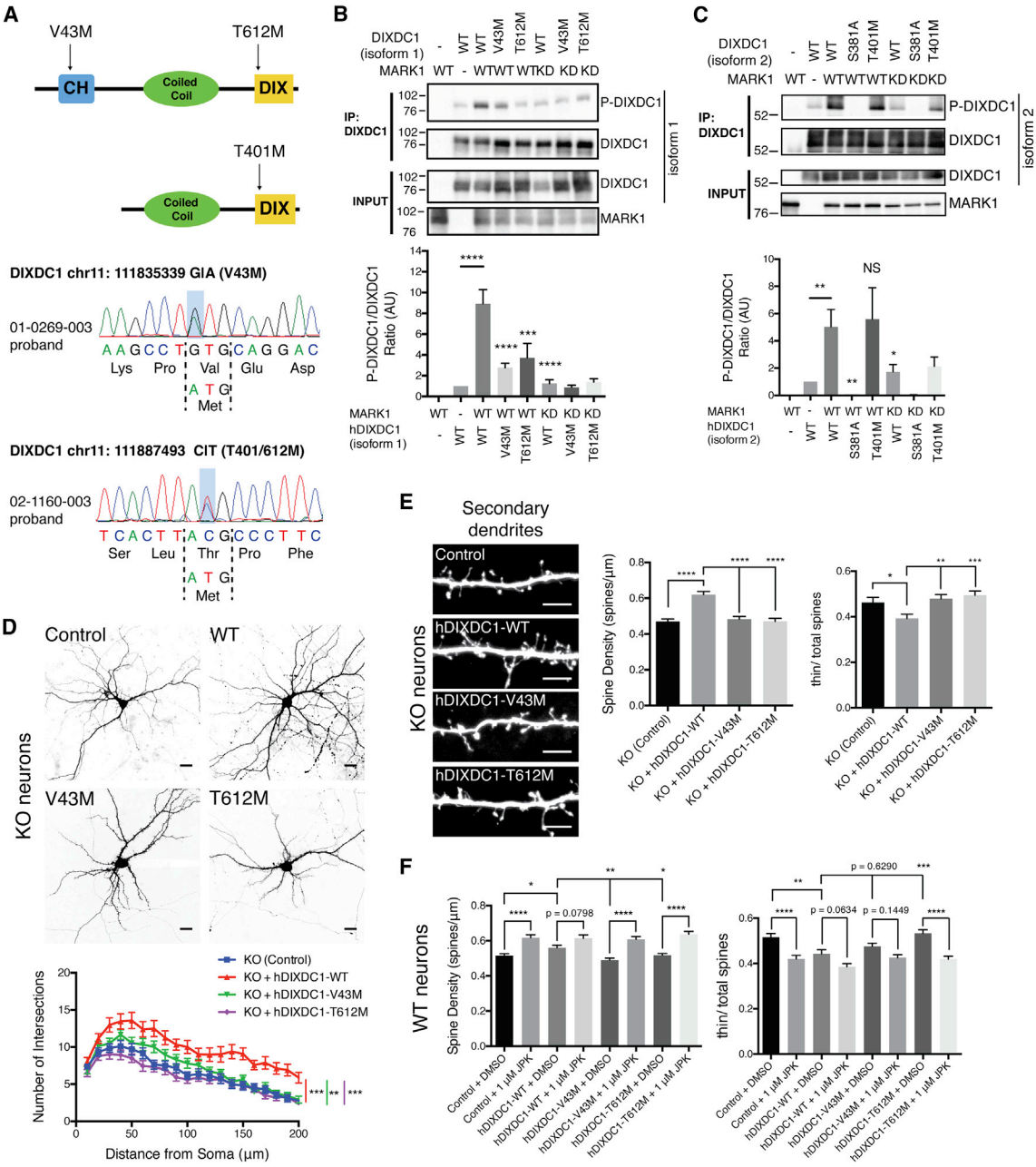

Figure 6. ASD-Linked Genetic Variants in *DIXDC1* Isoform 1 Impair Phosphorylation and Dendrite and Spine Growth

(A) Schematic diagram of DIXDC1 (isoform 1) shows the location of the V43M and T612M variants and confirmation by sequencing (family ID: 01-0269 [V43M] and 2-1160 [T612M]).

(B) Expression of hDIXDC1-V43M and -T612M in HEK293 cells results in a decrease in phosphorylation at DIXDC1 serine592 in the presence of MARK1 (n = 4; one-way ANOVA; post hoc Sidak test: ***p < 0.001; ****p < 0.0001).

(C) Expression of hDIXDC1 T401M in HEK293 cells does not affect phosphorylation at DIXDC1 serine381 (n = 3; one-way ANOVA; post hoc Sidak test: *p < 0.05; **p < 0.01).

(D) Sholl analysis of neurons expressing hDIXDC1-V43M and -T612M variants in KO neurons did not reveal an increase in dendritic tree complexity (KO; n = 3 cultures; two-way ANOVA; post hoc Sidak test: **p < 0.01; ***p < 0.001).

(E) Morphological analysis of neurons overexpressing hDIXDC1-V43M and -T612M in KO neurons did not show an increase in spine density compared to KO (control; n = 3 cultures; one-way ANOVA; post hoc Sidak test: *p < 0.05; **p < 0.01; ***p < 0.001; ****p < 0.0001).

(F) Morphological analysis of WT neurons expressing hDIXDC1-WT, -V43M, or -T612M and treated with JPK shows a rescue in defects in spine density (n = 3 cultures; one-way ANOVA; post hoc Sidak test: *p < 0.05; **p < 0.01; ***p < 0.001; ****p < 0.0001).

All numerical data are given as mean ± SEM. The scale bars represent 20 μm for (E) and 5 μm for (F). See also Figure S7. Refer to Supplemental Experimental Procedures and Figure S8 for details on image acquisition and analysis.

that both the N- and C-terminal domains of isoform 1 regulate the cytoskeleton, consistent with the actin-binding domain being present only in isoform 1 (Capelluto et al., 2002; Wang et al., 2006). This could also explain why isoform 2 does not have a strong direct impact on the actin and microtubule networks. Another potential explanation for the functional difference between the isoforms is that an unknown kinase could activate isoform 1 at threonine-612, acting as a priming site for serine-592 phosphorylation by MARK1. Alternatively, the threonine-401 site in isoform 2 could be regulated by a different kinase than MARK1. Given that isoform 2 can activate Wnt/β-catenin signaling (Shiomi et al., 2003), it may act via this pathway to regulate dendrite and synapse growth; however, it is unclear how isoform 2 activation of Wnt/β-catenin transcriptional signaling would result in local synaptic growth. In this regard, future studies should examine whether there is cross talk between the MARK1-cytoskeleton pathway and Wnt/β-catenin signaling.

DIXDC1 Signaling in ASDs and the Role of *DIXDC1* Missense Variants

In the current study, the biological interrogation of *DIXDC1* variants suggests that its function could be impaired in ASDs. One unresolved finding is that the V43M and T401/612M variants occur in putative healthy individuals, and the T612M was found in a homozygous state in two controls (Lek et al., 2016). Therefore, although the V43M and T612/401M variants have strong effects on DIXDC1 protein function, it is unclear how they contribute to disease risk. Furthermore, in our study, the T612M variant was inherited from parents who do not have ASD. However, it is not uncommon for unaffected family members to carry high-risk ASD mutations (Berkel et al., 2010). Whereas our data should be interpreted with caution, one potential explanation is the *DIXDC1* variants on their own are not sufficient to cause disease, but they interact with other variants to increase disease risk (Bourgeron, 2015). By contrast, protective factors could also be at play in the unaffected parents or the healthy controls that abrogate the effects of the *DIXDC1* variants.

Taken together, we reveal that MARK1-DIXDC1 signaling regulates developmental neural connectivity, which is disrupted by rare genetic variants in *DIXDC1*. This underscores the need to study DIXDC1 in normal and abnormal brain developmental paradigms to obtain a more complete understanding of its function.

EXPERIMENTAL PROCEDURES

Generation of *DIXDC1* Knockout Mouse and Animal Experiments

The *Dixdc1* KO mouse was generated by the Knockout Mouse Phenotyping Consortium. All mice were bred and maintained in the Central Animal Facility at McMaster University. All procedures received the approval of the Animal Research Ethics Board. Rat experiments were performed according to the German and European Animal Welfare Act and with the approval of local authorities of the city-state Hamburg (Behörde für Gesundheit und Verbraucherschutz, Fachbereich Veterinärwesen) and the animal care committee of the University Medical Center Hamburg-Eppendorf. Consent was obtained from all human participants, as approved by the Research Ethics Boards at The Hospital for Sick Children, McMaster University, and Memorial Hospital.

Primary Neuronal Cultures

Cortical neuron cultures were prepared from *Dixdc1* KO mouse, C57BL/6 (Charles River Laboratories), or CD-1 (Charles River) mouse E16 embryos as described previously (Johe et al., 1996). Cells were plated at a density of 5–7.5 × 10^5 cells per well onto coverslips coated with poly-D-lysine (BD Biosciences) and laminin (Sigma) in plating media (Neurobasal media [NB] [Invitrogen] + 10% fetal bovine serum [FBS] [GIBCO] + penicillin/streptomycin [Invitrogen], glutamine). After 1.5 hr, media was changed to culturing media (NB + B27 [Invitrogen] + penicillin [pen]/streptomycin [strep], L-glutamine [Invitrogen]). Cultures were treated with 1 μM cytosine arabinose (Ara-C) (Sigma) at DIV3/4.

Plasmid Transfections

Primary neuronal cultures (DIV7) were transfected with 1 μg of DNA for 6 hr in Neurobasal medium with Lipofectamine LTX according to the manufacturer's protocol (Life Technologies). Medium was changed to conditioned medium after 6 hr. HEK293FT cells were grown to 50%–70% confluence in DMEM with 10% fetal bovine serum and penicillin/streptomycin. Cells were transfected with appropriate DNA in DMEM without antibiotics using Lipofectamine 2000 according to manufacturer's protocol (Life Technologies). Cells were ~95% confluent at the time of harvesting.

Golgi Staining of Mouse Brains

Golgi staining was performed on P30 mouse brains using a commercial kit and protocol (FD Rapid GolgiStain Kit; FD NeuroTechnologies). Stained brains were imaged using Zeiss Axiocam ICm1 microscope camera. z stacks were acquired at 1-μm intervals and processed using ImageJ software (Sholl Analysis plugin).

Electrophysiological Recordings

Coronal brain slices (400 μm) were prepared in cold sucrose-based slicing solution containing (in mM): 160 sucrose; 2.5 KCl; 10 $MgSO_4$; 1.25 NaH_2PO_2; 25 glucose; 30 $NaHCO_3$; 20 HEPES; 5 Na-ascorbate; 3 Na-pyruvate; 2 thiourea; and 0.5 $CaCl_2$. Slices recovered for 45 min at 30°C and 45 min at room temperature. Whole-cell recordings (BX51WI; Olympus) were performed using an Axoclamp 700B amplifier (Molecular Devices) from patch electrodes (P-97 puller; Sutter Instruments) containing a cesium-based intracellular solution (in mM): 100 CsCl; 100 gluconic acid; 10 HEPES; 0.5 EGTA; 10 Na-phosphocreatine; 2 MgATP; and 0.5 NaGTP (pH 7.3). Brain slices were continuously superfused in artificial cerebrospinal fluid (aCSF) and a mix of 95% O2/5% CO2. Composition of aCSF was (in mM): 120 NaCl; 2.5 KCl; 1 MgSO4; 26 NaHCO3; 10 glucose; and 2 $CaCl_2$. One micromolar TTX and 100 μM picrotoxin were added to the bathing medium to block Na-dependent action potentials and GABA currents, respectively. Recordings were performed at −70 mV using Clampex 10.6 (Molecular Devices), corrected for a calculated −10 mV junction potential and analyzed using the Template Search function from Clampfit 10.6 (Molecular Devices).

Epi-fluorescence Time-Lapse Imaging

Epi-fluorescence time-lapse imaging was performed on an inverted Nikon microscope (Eclipse; Ti). During time-lapse imaging, cells plated on glass-bottomed culture chamber (Sarstedt) were kept in an acrylic chamber at 37°C in 5% CO_2. Light intensity of each channel was set at 1 or 2, with exposure time of 500–700 ms. Images were captured with CoolSNAP HQ2camera (Roper Scientific) using NIS-Elements AR software (Nikon). Images were captured every 1 or 2 s during the total 300-s interval.

Analysis of Dendrite Complexity and Dendritic Spine Density

Quantitative analysis of all dendrite complexity and spine density was performed using ImageJ software. Neurons expressing GFP were imaged using a confocal microscope (Zeiss, LSM700). Images for Sholl analysis were acquired using a 20× objective lens. Sholl analysis parameters were as follows: starting radius, 10 μm; ending radius, 100 μm; step size, 10 μm. Refer to Supplemental Experimental Procedures for detailed description of Sholl analysis. Spine density and morphology were measured from secondary branches, from the branch point, ranging from 15–25 μm in length. z stack images were acquired using a 63× oil immersion objective lens, and using two-dimensional maximum projection images, spine density was measured in ImageJ software. Statistics were performed using Prism statistical package (GraphPad).

Statistical Analysis

Compiled data are expressed as mean ± SEM. We used the two-tailed Student's t test, one-way ANOVA, and two-way ANOVA, with post hoc Sidak tests for statistical analyses (as indicated). The p values in the Results are from t tests unless specified otherwise. $p < 0.05$ was considered statistically significant. See Supplemental Information for detailed statistical methods (including two-way ANOVA statistical analysis to measure dendrite complexity).

ACCESSION NUMBERS

The accession numbers for the sequence data reported in this paper are EGA: EGAS00001001023 and EGAS00001000556.

SUPPLEMENTAL INFORMATION

Supplemental Information includes Supplemental Experimental Procedures, seven figures, and five movies and can be found with this article online at http://dx.doi.org/10.1016/j.celrep.2016.10.047.

AUTHOR CONTRIBUTIONS

V.K. and K.K.S. designed the experiments. V.K. performed neuronal cultures, transfections, and all biochemical experiments, with assistance from N.M., C.M., K.H., N.T.H., and B.K.U. The generation of GFP-tagged plasmids was performed by N.T.H., who is supervised by K.J.H. D.P.M. and B.S. are supervised by F.C.d.A. and completed live imaging experiments. K.K.S. performed viral injections. S.H.W. performed electrophysiology. C.L.H. performed initial live imaging experiments and is supervised by R.T. S.W. and R.K.C.Y. performed sequencing analysis and are supervised by S.W.S. Figures were prepared by V.K. and K.K.S. The manuscript was written by V.K. and K.K.S.

ACKNOWLEDGMENTS

We thank Dr. Reuben Shaw for providing reagents and Dr. Li-Huei Tsai for strong mentorship and support. This work was supported by grants to K.K.S. (Natural Sciences and Engineering Research Council, Bickell Medical Foundation, Scottish Rite Charitable Foundation, Krembil Foundation, Brain Canada Platform Support Grant, the Ontario Brain Institute [OBI], and the Canadian Institutes of Health Research [CIHR]), S.W.S. (OBI and CIHR), K.J.H. (CIHR and the Ontario Institute of Cancer Research), and R.T. (CIHR, Krembil, and CHDI Foundations). F.C.d.A. is supported by Deutsche Forschungsgemeinschaft (DFG) Grant (FOR 2419; CA1495/1-1), ERA-NET Neuron Grant (Bundesministerium für Bildung und Forschung [BMBF]; 01EW1410 ZMNH AN B1), Landesforschungsförderung Hamburg (Z-AN LF), and University Medical Center Hamburg-Eppendorf (UKE).

Received: February 11, 2016
Revised: September 2, 2016
Accepted: October 14, 2016
Published: November 8, 2016

REFERENCES

Berkel, S., Marshall, C.R., Weiss, B., Howe, J., Roeth, R., Moog, U., Endris, V., Roberts, W., Szatmari, P., Pinto, D., et al. (2010). Mutations in the SHANK2 synaptic scaffolding gene in autism spectrum disorder and mental retardation. Nat. Genet. *42*, 489–491.

Bourgeron, T. (2015). From the genetic architecture to synaptic plasticity in autism spectrum disorder. Nat. Rev. Neurosci. *16*, 551–563.

Brennand, K.J., Simone, A., Jou, J., Gelboin-Burkhart, C., Tran, N., Sangar, S., Li, Y., Mu, Y., Chen, G., Yu, D., et al. (2011). Modelling schizophrenia using human induced pluripotent stem cells. Nature *473*, 221–225.

Cao, F., Yin, A., Wen, G., Sheikh, A.M., Tauqeer, Z., Malik, M., Nagori, A., Schirripa, M., Schirripa, F., Merz, G., et al. (2016). Retraction note: alteration of astrocytes and Wnt/β-catenin signaling in the frontal cortex of autistic subjects. J. Neuroinflammation *13*, 106.

Capelluto, D.G., Kutateladze, T.G., Habas, R., Finkielstein, C.V., He, X., and Overduin, M. (2002). The DIX domain targets dishevelled to actin stress fibres and vesicular membranes. Nature *419*, 726–729.

Chen, J.A., Peñagarikano, O., Belgard, T.G., Swarup, V., and Geschwind, D.H. (2015). The emerging picture of autism spectrum disorder: genetics and pathology. Annu. Rev. Pathol. *10*, 111–144.

Ciani, L., Marzo, A., Boyle, K., Stamatakou, E., Lopes, D.M., Anane, D., McLeod, F., Rosso, S.B., Gibb, A., and Salinas, P.C. (2015). Wnt signalling tunes neurotransmitter release by directly targeting Synaptotagmin-1. Nat. Commun. *6*, 8302.

De Rubeis, S., Pasciuto, E., Li, K.W., Fernández, E., Di Marino, D., Buzzi, A., Ostroff, L.E., Klann, E., Zwartkruis, F.J., Komiyama, N.H., et al. (2013). CYFIP1 coordinates mRNA translation and cytoskeleton remodeling to ensure proper dendritic spine formation. Neuron *79*, 1169–1182.

De Rubeis, S., He, X., Goldberg, A.P., Poultney, C.S., Samocha, K., Cicek, A.E., Kou, Y., Liu, L., Fromer, M., Walker, S., et al.; DDD Study; Homozygosity Mapping Collaborative for Autism; UK10K Consortium (2014). Synaptic, transcriptional and chromatin genes disrupted in autism. Nature *515*, 209–215.

Dolan, B.M., Duron, S.G., Campbell, D.A., Vollrath, B., Shankaranarayana Rao, B.S., Ko, H.Y., Lin, G.G., Govindarajan, A., Choi, S.Y., and Tonegawa, S. (2013). Rescue of fragile X syndrome phenotypes in Fmr1 KO mice by the small-molecule PAK inhibitor FRAX486. Proc. Natl. Acad. Sci. USA *110*, 5671–5676.

Duffney, L.J., Wei, J., Cheng, J., Liu, W., Smith, K.R., Kittler, J.T., and Yan, Z. (2013). Shank3 deficiency induces NMDA receptor hypofunction via an actin-dependent mechanism. J. Neurosci. *33*, 15767–15778.

Duffney, L.J., Zhong, P., Wei, J., Matas, E., Cheng, J., Qin, L., Ma, K., Dietz, D.M., Kajiwara, Y., Buxbaum, J.D., and Yan, Z. (2015). Autism-like deficits in Shank3-deficient mice are rescued by targeting actin regulators. Cell Rep. *11*, 1400–1413.

Durand, C.M., Perroy, J., Loll, F., Perrais, D., Fagni, L., Bourgeron, T., Montcouquiol, M., and Sans, N. (2012). SHANK3 mutations identified in autism lead to modification of dendritic spine morphology via an actin-dependent mechanism. Mol. Psychiatry *17*, 71–84.

Ebert, D.H., and Greenberg, M.E. (2013). Activity-dependent neuronal signalling and autism spectrum disorder. Nature *493*, 327–337.

Fang, W.Q., Chen, W.W., Jiang, L., Liu, K., Yung, W.H., Fu, A.K., and Ip, N.Y. (2014). Overproduction of upper-layer neurons in the neocortex leads to autism-like features in mice. Cell Rep. *9*, 1635–1643.

Garcia, I., Huang, L., Ung, K., and Arenkiel, B.R. (2012). Tracing synaptic connectivity onto embryonic stem cell-derived neurons. Stem Cells *30*, 2140–2151.

Geschwind, D.H., and State, M.W. (2015). Gene hunting in autism spectrum disorder: on the path to precision medicine. Lancet Neurol. *14*, 1109–1120.

Goodwin, J.M., Svensson, R.U., Lou, H.J., Winslow, M.M., Turk, B.E., and Shaw, R.J. (2014). An AMPK-independent signaling pathway downstream of the LKB1 tumor suppressor controls Snail1 and metastatic potential. Mol. Cell *55*, 436–450.

Gu, J., Lee, C.W., Fan, Y., Komlos, D., Tang, X., Sun, C., Yu, K., Hartzell, H.C., Chen, G., Bamburg, J.R., and Zheng, J.Q. (2010). ADF/cofilin-mediated actin dynamics regulate AMPA receptor trafficking during synaptic plasticity. Nat. Neurosci. *13*, 1208–1215.

Han, K., Holder, J.L., Jr., Schaaf, C.P., Lu, H., Chen, H., Kang, H., Tang, J., Wu, Z., Hao, S., Cheung, S.W., et al. (2013). SHANK3 overexpression causes manic-like behaviour with unique pharmacogenetic properties. Nature *503*, 72–77.

Hayashi-Takagi, A., Takaki, M., Graziane, N., Seshadri, S., Murdoch, H., Dunlop, A.J., Makino, Y., Seshadri, A.J., Ishizuka, K., Srivastava, D.P., et al.

(2010). Disrupted-in-Schizophrenia 1 (DISC1) regulates spines of the glutamate synapse via Rac1. Nat. Neurosci. *13*, 327–332.

Hayashi-Takagi, A., Araki, Y., Nakamura, M., Vollrath, B., Duron, S.G., Yan, Z., Kasai, H., Huganir, R.L., Campbell, D.A., and Sawa, A. (2014). PAKs inhibitors ameliorate schizophrenia-associated dendritic spine deterioration in vitro and in vivo during late adolescence. Proc. Natl. Acad. Sci. USA *111*, 6461–6466.

Hori, K., Nagai, T., Shan, W., Sakamoto, A., Taya, S., Hashimoto, R., Hayashi, T., Abe, M., Yamazaki, M., Nakao, K., et al. (2014). Cytoskeletal regulation by AUTS2 in neuronal migration and neuritogenesis. Cell Rep. *9*, 2166–2179.

Huang, W., Zhu, P.J., Zhang, S., Zhou, H., Stoica, L., Galiano, M., Krnjević, K., Roman, G., and Costa-Mattioli, M. (2013). mTORC2 controls actin polymerization required for consolidation of long-term memory. Nat. Neurosci. *16*, 441–448.

Ikeuchi, Y., Stegmüller, J., Netherton, S., Huynh, M.A., Masu, M., Frank, D., Bonni, S., and Bonni, A. (2009). A SnoN-Ccd1 pathway promotes axonal morphogenesis in the mammalian brain. J. Neurosci. *29*, 4312–4321.

Iossifov, I., O'Roak, B.J., Sanders, S.J., Ronemus, M., Krumm, N., Levy, D., Stessman, H.A., Witherspoon, K.T., Vives, L., Patterson, K.E., et al. (2014). The contribution of de novo coding mutations to autism spectrum disorder. Nature *515*, 216–221.

Jeste, S.S., and Geschwind, D.H. (2014). Disentangling the heterogeneity of autism spectrum disorder through genetic findings. Nat. Rev. Neurol. *10*, 74–81.

Johe, K.K., Hazel, T.G., Muller, T., Dugich-Djordjevic, M.M., and McKay, R.D. (1996). Single factors direct the differentiation of stem cells from the fetal and adult central nervous system. Genes Dev. *10*, 3129–3140.

Kalkman, H.O. (2012). A review of the evidence for the canonical Wnt pathway in autism spectrum disorders. Mol. Autism *3*, 10.

Kivimäe, S., Martin, P.M., Kapfhamer, D., Ruan, Y., Heberlein, U., Rubenstein, J.L., and Cheyette, B.N. (2011). Abnormal behavior in mice mutant for the Disc1 binding partner, Dixdc1. Transl. Psychiatry *1*, e43.

Krumm, N., O'Roak, B.J., Shendure, J., and Eichler, E.E. (2014). A de novo convergence of autism genetics and molecular neuroscience. Trends Neurosci. *37*, 95–105.

Lei, W., Omotade, O.F., Myers, K.R., and Zheng, J.Q. (2016). Actin cytoskeleton in dendritic spine development and plasticity. Curr. Opin. Neurobiol. *39*, 86–92.

Lek, M., Karczewski, K.J., Minikel, E.V., Samocha, K.E., Banks, E., Fennell, T., O'Donnell-Luria, A.H., Ware, J.S., Hill, A.J., Cummings, B.B., et al.; Exome Aggregation Consortium (2016). Analysis of protein-coding genetic variation in 60,706 humans. Nature *536*, 285–291.

Mao, Y., Ge, X., Frank, C.L., Madison, J.M., Koehler, A.N., Doud, M.K., Tassa, C., Berry, E.M., Soda, T., Singh, K.K., et al. (2009). Disrupted in schizophrenia 1 regulates neuronal progenitor proliferation via modulation of GSK3beta/beta-catenin signaling. Cell *136*, 1017–1031.

Martin, P.M., Yang, X., Robin, N., Lam, E., Rabinowitz, J.S., Erdman, C.A., Quinn, J., Weiss, L.A., Hamilton, S.P., Kwok, P.Y., et al. (2013). A rare WNT1 missense variant overrepresented in ASD leads to increased Wnt signal pathway activation. Transl. Psychiatry *3*, e301.

Maussion, G., Carayol, J., Lepagnol-Bestel, A.M., Tores, F., Loe-Mie, Y., Milbreta, U., Rousseau, F., Fontaine, K., Renaud, J., Moalic, J.M., et al. (2008). Convergent evidence identifying MAP/microtubule affinity-regulating kinase 1 (MARK1) as a susceptibility gene for autism. Hum. Mol. Genet. *17*, 2541–2551.

Mohn, J.L., Alexander, J., Pirone, A., Palka, C.D., Lee, S.Y., Mebane, L., Haydon, P.G., and Jacob, M.H. (2014). Adenomatous polyposis coli protein deletion leads to cognitive and autism-like disabilities. Mol. Psychiatry *19*, 1133–1142.

Muhia, M., Thies, E., Labonté, D., Ghiretti, A.E., Gromova, K.V., Xompero, F., Lappe-Siefke, C., Hermans-Borgmeyer, I., Kuhl, D., Schweizer, M., et al. (2016). The kinesin KIF21B regulates microtubule dynamics and is essential for neuronal morphology, synapse function, and learning and memory. Cell Rep. *15*, 968–977.

Murakoshi, H., Wang, H., and Yasuda, R. (2011). Local, persistent activation of Rho GTPases during plasticity of single dendritic spines. Nature *472*, 100–104.

Okerlund, N.D., and Cheyette, B.N. (2011). Synaptic Wnt signaling-a contributor to major psychiatric disorders? J. Neurodev. Disord. *3*, 162–174.

Okerlund, N.D., Kivimäe, S., Tong, C.K., Peng, I.F., Ullian, E.M., and Cheyette, B.N. (2010). Dact1 is a postsynaptic protein required for dendrite, spine, and excitatory synapse development in the mouse forebrain. J. Neurosci. *30*, 4362–4368.

Penzes, P., Cahill, M.E., Jones, K.A., VanLeeuwen, J.E., and Woolfrey, K.M. (2011). Dendritic spine pathology in neuropsychiatric disorders. Nat. Neurosci. *14*, 285–293.

Reinhard, J.R., Kriz, A., Galic, M., Angliker, N., Rajalu, M., Vogt, K.E., and Ruegg, M.A. (2016). The calcium sensor Copine-6 regulates spine structural plasticity and learning and memory. Nat. Commun. *7*, 11613.

Riedl, J., Crevenna, A.H., Kessenbrock, K., Yu, J.H., Neukirchen, D., Bista, M., Bradke, F., Jenne, D., Holak, T.A., Werb, Z., et al. (2008). Lifeact: a versatile marker to visualize F-actin. Nat. Methods *5*, 605–607.

Riedl, J., Flynn, K.C., Raducanu, A., Gärtner, F., Beck, G., Bösl, M., Bradke, F., Massberg, S., Aszodi, A., Sixt, M., and Wedlich-Söldner, R. (2010). Lifeact mice for studying F-actin dynamics. Nat. Methods *7*, 168–169.

Shiomi, K., Uchida, H., Keino-Masu, K., and Masu, M. (2003). Ccd1, a novel protein with a DIX domain, is a positive regulator in the Wnt signaling during zebrafish neural patterning. Curr. Biol. *13*, 73–77.

Shiomi, K., Kanemoto, M., Keino-Masu, K., Yoshida, S., Soma, K., and Masu, M. (2005). Identification and differential expression of multiple isoforms of mouse Coiled-coil-DIX1 (Ccd1), a positive regulator of Wnt signaling. Brain Res. Mol. Brain Res. *135*, 169–180.

Singh, K.K., Ge, X., Mao, Y., Drane, L., Meletis, K., Samuels, B.A., and Tsai, L.H. (2010). Dixdc1 is a critical regulator of DISC1 and embryonic cortical development. Neuron *67*, 33–48.

Soma, K., Shiomi, K., Keino-Masu, K., and Masu, M. (2006). Expression of mouse Coiled-coil-DIX1 (Ccd1), a positive regulator of Wnt signaling, during embryonic development. Gene Expr. Patterns *6*, 325–330.

Sowers, L.P., Loo, L., Wu, Y., Campbell, E., Ulrich, J.D., Wu, S., Paemka, L., Wassink, T., Meyer, K., Bing, X., et al. (2013). Disruption of the non-canonical Wnt gene PRICKLE2 leads to autism-like behaviors with evidence for hippocampal synaptic dysfunction. Mol. Psychiatry *18*, 1077–1089.

Srikanth, P., Han, K., Callahan, D.G., Makovkina, E., Muratore, C.R., Lalli, M.A., Zhou, H., Boyd, J.D., Kosik, K.S., Selkoe, D.J., and Young-Pearse, T.L. (2015). Genomic DISC1 disruption in hiPSCs alters Wnt signaling and neural cell fate. Cell Rep. *12*, 1414–1429.

Tang, G., Gudsnuk, K., Kuo, S.H., Cotrina, M.L., Rosoklija, G., Sosunov, A., Sonders, M.S., Kanter, E., Castagna, C., Yamamoto, A., et al. (2014). Loss of mTOR-dependent macroautophagy causes autistic-like synaptic pruning deficits. Neuron *83*, 1131–1143.

Topol, A., Zhu, S., Tran, N., Simone, A., Fang, G., and Brennand, K.J. (2015). Altered WNT signaling in human induced pluripotent stem cell neural progenitor cells derived from four schizophrenia patients. Biol. Psychiatry *78*, e29–e34.

Turner, T.N., Sharma, K., Oh, E.C., Liu, Y.P., Collins, R.L., Sosa, M.X., Auer, D.R., Brand, H., Sanders, S.J., Moreno-De-Luca, D., et al. (2015). Loss of δ-catenin function in severe autism. Nature *520*, 51–56.

Um, K., Niu, S., Duman, J.G., Cheng, J.X., Tu, Y.K., Schwechter, B., Liu, F., Hiles, L., Narayanan, A.S., Ash, R.T., et al. (2014). Dynamic control of excitatory synapse development by a Rac1 GEF/GAP regulatory complex. Dev. Cell *29*, 701–715.

Wang, X., Zheng, L., Zeng, Z., Zhou, G., Chien, J., Qian, C., Vasmatzis, G., Shridhar, V., Chen, L., and Liu, W. (2006). DIXDC1 isoform, l-DIXDC1, is a novel

filamentous actin-binding protein. Biochem. Biophys. Res. Commun. *347*, 22–30.

Wen, Z., Nguyen, H.N., Guo, Z., Lalli, M.A., Wang, X., Su, Y., Kim, N.S., Yoon, K.J., Shin, J., Zhang, C., et al. (2014). Synaptic dysregulation in a human iPS cell model of mental disorders. Nature *515*, 414–418.

Woolfrey, K.M., and Srivastava, D.P. (2016). Control of dendritic spine morphological and functional plasticity by small GTPases. Neural Plast. *2016*, 3025948.

Wu, Q., DiBona, V.L., Bernard, L.P., and Zhang, H. (2012). The polarity protein partitioning-defective 1 (PAR-1) regulates dendritic spine morphogenesis through phosphorylating postsynaptic density protein 95 (PSD-95). J. Biol. Chem. *287*, 30781–30788.

Yuen, R.K., Thiruvahindrapuram, B., Merico, D., Walker, S., Tammimies, K., Hoang, N., Chrysler, C., Nalpathamkalam, T., Pellecchia, G., Liu, Y., et al. (2015). Whole-genome sequencing of quartet families with autism spectrum disorder. Nat. Med. *21*, 185–191.